International Journal of Heat and Mass Transfer 52 (2009) 2049–2058

Contents lists available at ScienceDirect

International Journal of Heat and Mass Transfer

journal homepage: www.elsevier.com/locate/ijhmt

Nonlinear optimal on-line heat-dissipation control methodology in electronic devices

Horng-Yuan Jang [a,*], Chung-Hsin Cheng [b]

[a] Department of Computer Science and Information Engineering, Nan Kai University of Technology, Taiwan, ROC
[b] Department of Power Vehicle and Systems Engineering, Chung Cheng Institute of Technology, National Defense University, Taiwan, ROC

ARTICLE INFO

Article history:
Received 21 June 2008
Received in revised form 5 November 2008
Available online 25 December 2008

Keywords:
Active thermal control
CPU cooling
Extended Kalman filter
Input estimation method
Inverse estimation
Linear quadratic Gaussian

ABSTRACT

The essential element in obtaining semiconductor electronic device enhanced reliability involves solving the heat-dissipating issue. Certain electronic components possess varying thermal properties and the strength of the heat generated by the semiconductor chip is unknown. Therefore, the heat dissipation control problem is both complicated and perplexing. This paper proposes a methodology, the LQG/IE tracking algorithm, to solve the nonlinear heat dissipation control problem. The IE method, which is a combination of an Extended Kalman filter and Recursive Least Squares Estimator, estimates (in real time) the unknown time-varying heat source generated by the semiconductor chip using temperature measurements of the package seal surface. The LQG tracking algorithm is adopted to analyze the feedback gain to control the heat dissipation. The simulation results reveal that an effective and optimal heat dissipation controller can be implemented for the cooling system using the LQG/IE tracking algorithm.

1. Introduction

Today's electronic devices have more effective computing capability. Aside from this, their light weight and small size provide portability. However, sufficiently dealing with the thermal effect is essential to the previous research and development success. The heat produced during high-speed computer operations increases with the CPU calculation speed [1]. The lifetime and reliability of electronic components fall as the operating temperature increases [2,3]. And also, the thermal properties of the chip package seal module changed with temperatures [4]. Consequently, controlling the temperature of these components is the best way to increase the lifespan of electronic products. Some electronic components have thermal properties that vary quickly with temperature changes during operation. The strength of the heat generated by the semiconductor chip is unknown. Therefore, the nonlinear heat dissipation control problem is both complicated and perplexing.

In past decades, many studies have been conducted on controlling the temperature rise in electronic devices [5–8]. These studies focused on reducing the interfacial thermal impedance, which may be called passive thermal control. Some active thermal control methods have been proposed to lift the limitations on passive thermal control methods [9–12]. Some involve feedback control systems [9,10], while others do not [11,12]. However, there are two difficult areas in feedback control system applications to heat dissipation in electronic devices. The first is the thermal time delay problem. The second is the short time period for control action. The main cause of these difficulties is poor prediction of the time-varying heat generated by the CPU. Thus, accurate real time estimation of the time-varying heat generated by the CPU plays an important role in active thermal control methods.

In the past, much research on the optimal control design problem focused on well defined systems. This means that all system parameters are given initially and the system input is also well known. Under these conditions, the LQG regulator [13] could easily solve the optimization problem with good accuracy. However, it is difficult to obtain a good solution for heat dissipation control design if the thermal input is deterministic but uncertain. Accordingly, the approach proposed here involves a combined control algorithm that could concurrently estimate unknown thermal input on-line using the IE method and solve the optimal control problem based on the LQG tracking algorithm.

When the heat produced during operation is unknown, it can be estimated inversely by applying temperature measurements on the boundary. The real-time inverse estimation method in the past focused mostly on linear heat conduction systems. In 1996, Tuan et al. [14] proposed the On-line input estimation (IE) method to estimate the unknown heat flux in a linear inverse heat conduction problem (IHCP). The linear IHCP was addressed by Tuan and co-workers [15,16]. In practical

* Corresponding author. Tel.: +886 49 2563489x3266; fax: +886 49 2561408.
E-mail address: jghgyn@nkut.edu.tw (H.-Y. Jang).

0017-9310/$ - see front matter © 2008 Elsevier Ltd. All rights reserved.
doi:10.1016/j.ijheatmasstransfer.2008.11.002

Nomenclature

A	Jacobian matrices defined by Eq. (41a)
B	sensitivity matrix defined by Eq. (48)
C	volumetric heat capacity defined by Eq. (2)
$\overline{C}$	dimensionless volumetric heat capacity defined by Eq. (5)
C_p	specific heat of package seal, J kg^{-1} °C^{-1}
$E(\cdot)$	expected value
e	state variable error
F_θ	Jacobian matrices defined by Eq. (24)
$F_{\bar{\varphi}}$	Jacobian matrices defined by Eq. (25)
$F_{\bar{u}}$	Jacobian matrices defined by Eq. (26)
f	function matrix
g	adjoint vector defined by Eq. (37)
H	the measurement matrix defined by Eq. (42)
h	spatial interval
I	identity matrix
J_j	quadratic performance index function defined by Eq. (31)
K	Kalman gain defined by Eq. (46)
K_b	Kalman gain of input estimation defined by Eq. (50)
k,j	time (discrete)
k_f	time (discrete) for final time
L	thickness of package material, m
M	sensitivity matrix defined by Eq.(49)
N	total number of spatial nodes for $x = L$
P	filter's error covariance matrix defined by Eq. (47)
P_b	error covariance matrix defined by Eq. (51)
P_i	matrix defined by Eq. (35)
Q_c	weights of the control defined by Eq. (33)
Q_d	process noise covariance matrix
Q_0	weighting matrix of state variable error for final time
Q_s	weights of the state variable error defined by Eq. (32)
Q_1	weighting matrix of state variable error for overall process
R	measurement noise covariance
RMSE	root mean square error defined by Eq. (54)
s	innovation covariance defined by Eq. (45)
T	temperature (°C)
t	time (continuous) (s)
t_f	final time (s)
u	unknown boundary heat flux input control (W m^{-2})
$\bar{u}$	dimensionless boundary heat flux control input $(= Lu(t)/k_0(t_\infty - T_0))$
$\bar{u}_{\max}$	permission maximum control effort
ω	process noise vector
X	dimensionless spatial variable $(=x/L)$
x	axial coordinate (m)
z_m	observation state vector (°C)
z_m	dimensionless observation state vector
$\bar{z}$	Bias innovation defined by Eq. (44)

Greek symbols

α_0	thermal diffusivity $(=k_0/c_0)$
Γ	coefficient vector defined by Eq. (41c)
γ	memory factor
$\Delta\tau$	sampling time interval
δ	Dirac delta function
$\delta\theta$	perturbation state variable
η	random variable
θ	dimensionless temperature
$\dot{\theta}$	time derivative of the state vector
θ_d	design working temperature
θ_ε	maximum tolerance of temperature error
θ_p	temperature of package seal near chip
κ	thermal conductivity defined by Eq. (1)
$\bar{\kappa}$	dimensionless thermal conductivity defined by Eq. (6)
v	measurement noise vector (°C)
ρ	density of package seal (kg m^{-3})
σ	standard deviation
τ	dimensionless time $(=\alpha_0 t/L^2)$
τ_f	dimensionless final time $(=\alpha_0 t/L^2)$
Φ	state transition matrix defined by Eq. (41a)
$\varphi(t)$	strength of the heat source (W/m^3)
$\bar{\varphi}(\tau)$	dimensionless strength of the heat source $(=L^2\phi(t)/(k_0(T_\infty - T_0)))$
Ψ	coefficient matrix defined by Eq. (41b)

Subscripts

0	initial temperature
*	extensible controller
air	natural convection
exact	exact heat flux
∞	ambient temperature

Superscripts

^	estimated
T	transpose of matrix

conditions, the heat conduction process is mostly a nonlinear heat conduction problem. Meric in 1979 adopted the conjugate gradient method to optimally control a nonlinear boundary temperature distribution [17,18]. Chen and Ozisik applied a similar algorithm to the heat source estimation within plate [19,20] and cylinder systems [21]. Huang in 2001 used this algorithm to estimate the optimal heat flux control function in a nonlinear heat conduction problem [22]. Daouas and Radhouani [23] applied the smoothing technique associated with the extended Kalman filter to solve nonlinear one-dimensional IHCP. Chen and Wu [24] have applied the hybrid scheme in conjunction with a sequential-in-time concept, the Taylor series approximation, least-squares method, and actual experimental temperature data to estimate the unknown surface condition for the nonlinear IHCP. Loulou and Artioukhine [25] proposeed a numerical algorithm to solve a three-dimensional unsteady nonlinear IHCP of estimating surface heat flux for cylindrical geometry. Chen proposed the IE method to inversely estimate the unknown heat source in real time in a nonlinear heat conduction problem [26]. However, this method was not extended to solve the optimal thermal control problem. This research studies the optimal thermal control problem of a nonlinear heat-conducting system under the influence of unknown thermal input. The main objective of this work is to develop an adaptive control algorithm that predicts the optimal value of time-varying heat dissipation which must be removed by the cooling system, with the problem corrupted by modeled noise and unknown thermal input. After estimating the amount of heat that must be dissipated, an effective cooling system can then be designed to assure that the semiconductor chip will be operated within a safe temperature regime.

In this work, a nonlinear heat dissipation model is defined first for semiconductor electronic devices. An innovative controller that combines the LQG tracking algorithm and IE method is then developed to control the electronic device heat dissipation. Elaborate experiments are simulated for some cases, the results compared and conclusions drawn.

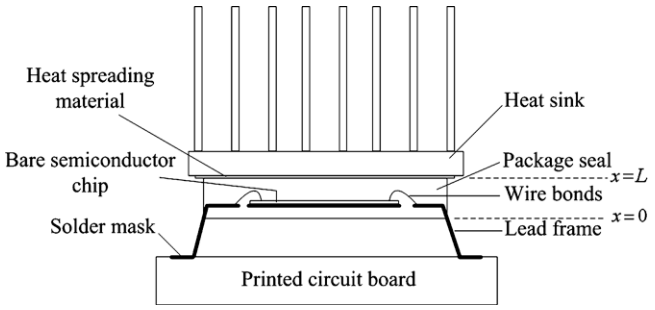

Fig. 1. Schematic diagram of surface mounted package of semiconductor electronic device.

2. Problem formulation

The problem considered is the conduction of heat through a package seal to heat-dissipation components during the operation of a semiconductor electronic device. Fig. 1 details a schematic diagram of a surface mounted semiconductor package within an electronic device. A bare semiconductor chip is attached to a lead frame, sealed with a solder mask and then mounted onto a printed circuit board. Heat spreading material is uniformly applied between the package seal and heat sink on top of the package seal. The heat sink is mounted directly onto the seal to improve the heat-dissipation efficiency.

To simplify the analysis, a one-dimensional heat conduction model is employed as outlined in Fig. 2. Consider a package seal that is a uniform thermal conductor with thickness, L. An unknown heat source, $\phi(t)$, generated by the semiconductor chip acts on the package seal at $x = x_b$. In fact, when the heat sink is mounted directly onto the top side of package seal, the heat is dissipated mostly through by top of package seal and heat sink, and the small part's quantity of heat will pass through lead frame to printed circuit board. In order to consider the maximized heat-dissipation design of the controller, a thermal insulated condition is assumed at bottom of the package seal at $x = 0$. The thermal conductivity coefficient $\kappa(T)$ and the volumetric heat capacity $\rho C_p(T)$ that will change with the variation in the temperature. The assumptions are made as follows:

$$\kappa(T) = k_0 + k_1(T - T_0) + k_2(T - T_0)^2 \tag{1}$$

$$C(T) = \rho C_p(T) = c_0 + c_1(T - T_0) + c_2(T - T_0)^2 \tag{2}$$

where T_0 is the initial temperature of the electronic component at time, $t = 0$. The one-dimensional transient nonlinear heat conduction problem can be defined as follows:

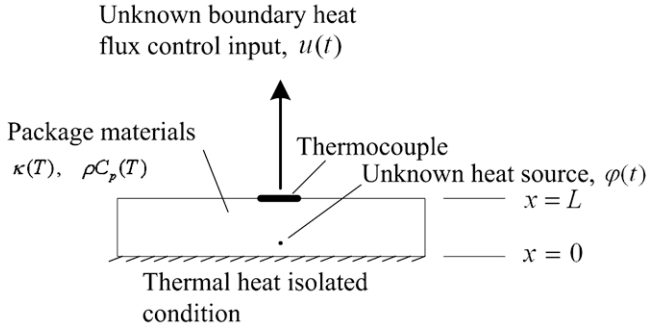

Fig. 2. A simplified heat-dissipation model of the nonlinear heat conduction problem.

$$\frac{\partial}{\partial x}\left[\kappa(T)\frac{\partial T(x,t)}{\partial x}\right]\varphi(t)\delta(x - x_b) = \rho C_p(T)\frac{\partial T(x,t)}{\partial t}, \quad 0 < x < L \quad 0 < t \leqslant t_f \tag{3a}$$

$$-\kappa(T)\frac{\partial T(x,t)}{\partial x} = 0, \qquad x = 0 \tag{3b}$$

$$-\kappa(T)\frac{\partial T(x,t)}{\partial x} = u(t), \qquad x = L \tag{3c}$$

$$T(x,0) = T_0 \tag{3d}$$

where $T(x,t)$ is temperature field distribution as a function of x and t. $\varphi(t)$ is an unknown heat source applied at the position, $x = x_b$. $u(t)$ is unknown boundary heat flux control input.

The measured temperature, $z_m(t)$, is obtained from the thermocouple at the top side of package seal, $x = l$. The measurement equation is defined as follows:

$$z_m(t) = T(x,t) + v(t) \qquad x = L \tag{4}$$

where $v(t)$ is the measurement error, which is assumed to be the Gaussian white noise with zero mean.

For computation convenience, Eqs. (3a)–(3d) and Eq. (4) of the nonlinear heat conduction problem are transferred into the dimensionless forms as follows:

$$\bar{C} = C/c_0 = 1 + \bar{c}_1\theta + \bar{c}_2\theta, \quad \bar{c}_1 = \frac{c_1(T_\infty - T_0)}{c_0}, \quad \bar{c}_2 = \frac{c_2(T_\infty - T_0)^2}{c_0}, \quad \theta = \frac{T - T_0}{T_\infty - T_0} \tag{5}$$

$$\bar{\kappa} = \frac{\kappa}{k_0} = 1 + \bar{k}_1\theta + \bar{k}_2\theta^2, \quad \bar{k}_1 = \frac{k_1(T_\infty - T_0)}{k_0}, \quad \bar{k}_2 = \frac{k_2(T_\infty - T_0)^2}{k_0} \tag{6}$$

and

$$\frac{\partial T}{\partial t} = (T_\infty - T_0)\frac{\alpha_0}{L^2}\frac{\partial\theta}{\partial\tau} \tag{7}$$

$$\frac{\partial T}{\partial x} = \frac{(T_\infty - T_0)}{L}\frac{\partial\theta}{\partial X} \tag{8}$$

By substituting Eqs. (5)–(8), into Eqs. (3a)–(3d), and Eq. (4), the dimensionless nonlinear energy equations can be written as

$$\frac{\partial\theta}{\partial\tau} = \frac{1}{\bar{C}(\theta)}\frac{\partial}{\partial X}\left[\bar{\kappa}(\theta)\frac{\partial\theta}{\partial x}\right] + \frac{1}{\bar{C}(\theta)}\bar{\varphi}(\tau)\delta(X - X_b) \tag{9}$$

The associated boundary conditions the initial condition are taken as

$$\bar{\kappa}(\tau)\frac{\partial\theta(X,\tau)}{\partial X} = 0, \qquad X = 0, \quad \tau > 0 \tag{10}$$

$$-\bar{\kappa}(\tau)\frac{\partial\theta(X,\tau)}{\partial X} = \bar{u}(\tau), \qquad X = 1,, \quad \tau > 0 \tag{11}$$

$$\theta(X,0) = 1, \quad 0 \leqslant X \leqslant 1 \tag{12}$$

with measurements

$$Z(\tau) = \frac{z_m(t) - T_0}{T_\infty - T_0} \tag{13}$$

Based on the central difference method [27], there are N nodes from $X = 0$ to $X = 1$, and assume that the spatial interval $h = 1/(N - 1)$. Let θ_1 be the temperature at node 1, which is at the position, $X = 0$, the boundary conditions of Eqs. (10) and (11), and the dimensionless energy equation can be written as

$$\frac{\partial\theta}{\partial\tau} = \frac{\bar{k}_1 + 2\bar{k}_2\theta}{\bar{C}(\theta)}\left(\frac{\partial\theta}{\partial X}\right)^2 + \frac{\bar{\kappa}\theta}{\bar{C}(\theta)}\frac{\partial^2\theta}{\partial X^2} + \frac{\bar{\varphi}(\tau)}{\bar{C}(\theta)}\delta(X - X_b) \tag{14}$$

From central difference approximation, we know that

$$\frac{\partial\theta_i}{\partial X}=\frac{\theta_{i+1}-\theta_{i-1}}{2h},\quad \frac{\partial^2\theta}{\partial X^2}=\frac{\theta_{i+1}-2\theta_i+\theta_{i-1}}{h^2} \tag{15}$$

By choosing $i=1$, substituting Eq. (15) into Eq. (14), and consider the boundary condition, Eq. (10), we can get

$$\dot{\theta}_1(\tau)=f_1=\frac{\bar{\kappa}(\theta_1)}{\bar{C}(\theta_1)}\frac{2\theta_2-2\theta_1}{h^2}+\frac{\bar{\varphi}(\tau)}{\bar{C}(\theta_1)}\delta(X-X_b) \tag{16}$$

By applying $i=2,3,\ldots,N-1$, to Eqs. (14) and (15), we can get

$$\dot{\theta}_1(\tau)=f_1=\frac{(\bar{k}_1 2\bar{k}_2\theta_i)}{\bar{C}(\theta_i)}\left(\frac{\theta_{i+1}-\theta_{i-1}}{2h}\right)^2\frac{\bar{\kappa}(\theta_i)}{\bar{C}(\theta_i)}\left(\frac{\theta_{i+1}-2\theta_i+\theta_{i-1}}{h^2}\right)+\frac{\bar{\varphi}(t)}{\bar{C}(\theta_i)}\delta(X-X_b) \tag{17}$$

Choosing $i=N$, substituting Eq. (15) into Eq. (14), and consider the boundary condition, Eq. (11), we can get

$$\dot{\theta}_N(\tau)=f_N=\frac{2h\bar{u}^2(\bar{k}_1+2\bar{k}_2\theta_N)}{\bar{\kappa}(\theta_N)\bar{C}(\theta_N)}+\frac{\bar{\kappa}(\theta_N)}{\bar{C}(\theta_N)}\left(\frac{2\theta_{N-1}-2\theta_N}{h^2}\right)-\frac{2\bar{q}}{h\bar{C}(\theta_N)}+\frac{\bar{\varphi}(\tau)}{\bar{C}(\theta_N)}\delta(X-X_b) \tag{18}$$

By combining Eq. (16) to Eq. (18) and taking the process noise input into account, the nonlinear continuous-time state equation can be derived as follows:

$$\dot{\theta}(\tau)=f[\theta(\tau),\bar{\varphi}(\tau),\bar{u}(\tau),\tau]+\omega(\tau) \tag{19}$$

where

$$\theta(\tau)=[\theta_1(\tau),\theta_2(\tau),\ldots,\theta_N(\tau)]^T$$
$$f=[f_1,f_2,\ldots,f_N]^T$$
$$\omega(\tau)=[\omega_1,\omega_2,\ldots,\omega_N]^T$$

where $\dot{\theta}(\tau)$ is short for $d\theta(\tau)/d\tau$, and $\omega(\tau)$ is white process noise.

Given a nominal input, $\bar{\varphi}^*(\tau)$, nominal control input, $\bar{u}^*(\tau)$, and the nominal temperature, $\theta^*(\tau)$, will satisfy the nominal system as follows:

$$\dot{\theta}^*(\tau)=f[\theta^*(\tau),\bar{\varphi}^*(\tau),\bar{u}^*(\tau),\tau] \tag{20}$$

Let

$$\delta\theta(\tau)=\theta(\tau)-\theta^*(\tau),\quad \delta\bar{\varphi}(\tau)=\bar{\varphi}(\tau)-\bar{\varphi}^*(\tau),$$
$$\delta\bar{u}(\tau)=\bar{u}(\tau)-\bar{u}^*(\tau) \tag{21}$$

then

$$\frac{d}{d\tau}\delta\theta(\tau)=\delta\dot{\theta}(\tau)=\dot{\theta}(\tau)-\dot{\theta}(\tau)=f[\theta(\tau),\bar{\varphi}(\tau),\bar{u}(\tau),\tau]+G(\tau)\omega(\tau)-f[\theta^*(\tau),\bar{\varphi}^*(\tau),\bar{u}^*(\tau),\tau] \tag{22}$$

Expanding $f[\theta(\tau),\bar{\varphi}(\tau),\bar{u}(\tau),\tau]$ in Taylor series with respect to $\theta^*(\tau),\bar{\varphi}^*(\tau),\bar{u}^*(\tau)$, and neglecting the higher-order terms, considering the uncertainties and disturbances in real electronic devices, the input process noise is added into the unknown heat source term $\bar{\varphi}(\tau)$, the following perturbation equation can be obtained:

$$\begin{aligned}\delta\dot{\theta}(\tau)&=F_\theta[\theta^*(\tau),\bar{\varphi}^*(\tau),\bar{u}^*(\tau),\tau]\delta\theta(\tau)\\&\quad+F_{\bar{\varphi}}[\theta^*(\tau),\bar{\varphi}^*(\tau),\bar{u}^*(\tau),\tau]\delta\bar{\varphi}(\tau)\\&\quad+F_{\bar{u}}[\theta^*(\tau),\bar{\varphi}^*(\tau),\bar{u}^*(\tau),\tau]\delta\bar{u}(\tau)\\&\quad+F_{\bar{\varphi}}[\theta^*(\tau),\bar{\varphi}^*(\tau),\bar{u}^*(\tau),\tau]\omega(\tau)\end{aligned} \tag{23}$$

where $F_\theta, F_{\bar{\varphi}}$ and $F_{\bar{u}}$ are $N\times N$, $N\times 1$ and $N\times 1$ Jacobian matrices, respectively.

$$F_\theta[\theta^*(\tau),\bar{\varphi}^*(\tau),\bar{u}^*(\tau),\tau]=\begin{bmatrix}\frac{\partial f_1}{\partial\theta_1^*} & \cdots & \frac{\partial f_1}{\partial\theta_N^*}\\ \vdots & \ddots & \vdots\\ \frac{\partial f_N}{\partial\theta_1^*} & \cdots & \frac{\partial f_N}{\partial\theta_N^*}\end{bmatrix} \tag{24}$$

$$F_{\bar{\varphi}}[\theta^*(\tau),\bar{\varphi}^*(\tau),\bar{u}^*(\tau),\tau]=\left[\frac{\partial f_1}{\partial\bar{\varphi}^*}\cdots\frac{\partial f_N}{\partial\bar{\varphi}^*}\right]^T \tag{25}$$

$$F_{\bar{u}}[\theta^*(\tau),\bar{\varphi}^*(\tau),\bar{u}^*(\tau),\tau]=\left[\frac{\partial f_1}{\partial\bar{u}^*}\cdots\frac{\partial f_N}{\partial\bar{u}^*}\right]^T \tag{26}$$

This work develops an innovative controller using an LQG/IE tracking algorithm that can determine the amount of heat dissipated, $\bar{u}(\tau)$, under unknown heat source, $\bar{\varphi}(\tau)$.

3. The algorithm of IE method combined with LQG tracking algorithm

Based on the assumption that the heat source, $\bar{\varphi}(\tau)$, is zero or a known value in Eq. (19), an optimal control result can be obtained using the LQG regulator. However, when the system that is being controlled has a time-varying heat source, $\bar{\varphi}(\tau)$, such as the heat source resulting from electronic device operation, the optimal heat-dissipating control system design for the time-varying heat source cannot easily be obtained using an LQG regulator. To resolve this issue, this work proposes a combined control theorem that utilizes the separation principle [13] in the calculation. The control problem is divided into two portions - optimal control and parameter estimation. In solving the optimal control problem, heat-dissipating control quantity, $\bar{u}(\tau)$, is estimated using the LQG tracking algorithm, and then in solving parameter estimation problems, the heat source input variable, $\bar{\varphi}(\tau)$, is then estimated using the IE method.

For controller design, the continue-time perturbation state equation and the measurement equation are given using

$$\delta\dot{\theta}(\tau)=F_\theta\delta(\theta)(\tau)+F_{\bar{\varphi}}\delta\bar{\varphi}(\tau)+F_{\bar{u}}\delta\bar{u}(\tau)+F_{\bar{\varphi}}\omega(\tau) \tag{27}$$
$$z(\tau)=H\theta(\tau)+v(\tau) \tag{28}$$

where F_θ short for $F_\theta[\theta^*(\tau),\bar{\varphi}^*(\tau),\bar{u}^*(\tau),\tau], F_{\bar{\varphi}}$ short for $F_{\bar{\varphi}}[\theta^*(\tau),\bar{\varphi}^*(\tau),\bar{u}^*(\tau),\tau]$, and $F_{\bar{u}}$ short for $F_{\bar{u}}[\theta^*(\tau),\bar{\varphi}^*(\tau),\bar{u}^*(\tau),\tau]$, and rearrange of Eq. (27), we can get

$$\delta\bar{\theta}(\tau)=F_\theta\cdot\delta\theta(\tau)+F_{\bar{u}}\left[\delta\bar{u}(\tau)+\left(F_{\bar{u}}^TF_{\bar{u}}\right)^{-1}F_{\bar{u}}^TF_{\bar{\varphi}}\delta\bar{\varphi}(\tau)\right]+F_{\bar{\varphi}}w(\tau) \tag{29}$$

Let the items in parentheses in Eq. (29) represent the deviation of extensible controller, $\delta\bar{u}_*(\tau)$ and the following equation can then be obtained.

$$\delta\dot{\theta}(\tau)=F_\theta\delta\theta(\tau)+F_{\bar{u}}\delta\bar{u}_*(\tau)+F_{\bar{\varphi}}w\tau \tag{30}$$

The quadratic performance index, $J_i(\bar{u})_*$ is defined as

$$J_i(\bar{u}_*)=E\left[\frac{1}{2}e^T(\tau_f)Q_0(\tau)e(\tau_f)+\frac{1}{2}\int_{\tau_0}^{\tau_f-\Delta\tau}\left[e^T(\tau)Q_1(\tau)e(\tau)+\bar{u}_*^T(\tau)Q_c(\tau)\bar{u}_*\right]d\tau\right] \tag{31}$$

where $\bar{u}_*(\tau) = \bar{u}_*^*(\tau) + \delta\bar{u}_*(\tau)$ and $e(\tau) = \theta_p(\tau) - \theta_d(\tau), \bar{u}_*^*(\tau)$ is a reference extensible controller. Q_0 and Q_1 are nonnegative weighting scalars, and Q_c is a positive weighting scalar. The physical meanings of the terms in the quadratic performance index are as follows. $e^T(\tau_f)Q_0e(\tau_f)$ represents the temperature error at the final time and the other two terms specify the requirements for the temperature error and the control variable during the control process, which includes the error, $e^T(\tau)Q_1(\tau)e(\tau)$, and the control effort, $\bar{u}_*^T(\tau)Q_c(\tau)\bar{u}_*(\tau)$. $e^T(\tau)Q_1(\tau)e(\tau)$ and $\bar{u}_*^T(\tau)Q_c(\tau)\bar{u}_*(\tau)$ are interdependent. Reducing the temperature error requires the magnification of control effort, but which might not be obtained in practice if the value is too large. On the other hand, in order to reduce the control effort, the request for the reduction of temperature error will need to be compromised in a way. In this work, we set $Q_0 = Q_1 = Q_s$, Q_s and Q_c are defined as follows:

$$Q_s = \frac{1}{\theta_\epsilon} \tag{32}$$

$$Q_c \leqslant \frac{1}{\bar{u}_{\max}} \tag{33}$$

In this work, the value of θ_ε depends on the temperature error between the design working temperature and the temperature of the package seal near the chip. $\bar{u}_{\max}$ is an adjustable parameter in which the upper limit is the maximum chosen heat dissipation amount for the cooling system.The LQG tracking algorithm is used to optimize the feedback control vector, $\bar{u},(\tau)$, and can be rewritten as follows [28]:

$$\hat{\bar{u}}_* = -Q_c^{-1}(\tau)\cdot F_{\bar{u}}^T(\tau)\left[P_1(\tau)\hat{\theta}(\tau) - g(\tau)\right] \tag{34}$$

where $P_1(\tau)$ is the solution for the Ricatti equation with boundary conditions,

$$\begin{aligned}-\dot{P}(\tau) &= P_1(\tau)F_\theta(\tau) + F_\theta^T(t)P_1(\tau)\\ &\quad - P_1(\tau)F_{\bar{u}}(\tau)Q_c^{-1}(\tau)F_{\bar{u}}^T(\tau)P_1(\tau) + H^TQ_1(\tau)H\end{aligned} \tag{35}$$

$$P_1(\tau_f) = H^TQ_0H \tag{36}$$

In the meantime, $g(\tau)$ is the solution for the adjoining equation with boundary conditions:

$$-\dot{g}(\tau) = [F_\theta(\tau) - F_{\bar{u}}(\tau)Q_c^1(\tau)F_{\bar{u}}^T(\tau)P_1(\tau)]^Tg(\tau) + H^TQ_1(\tau)\theta_d(\tau) \tag{37}$$

$$g(\tau_f) = H^TQ_0\theta_d(\tau_f) \tag{38}$$

The optimal control $\bar{u}(\tau)$ can be written as

$$\hat{\bar{u}}(\tau) = -Q_c^{-1}(\tau)\cdot F_{\bar{u}}^T[P_1(\tau)\hat{\theta}(\tau) - g(\tau)] - (F_{\bar{u}}^TF_{\bar{u}})^{-1}F_{\bar{u}}^TF_{\bar{\varphi}}\hat{\bar{\varphi}}(\tau) \tag{39}$$

The last term in Eq. (39) is a compensation for heat generated by the heat source, the value of heat source $\hat{\bar{\varphi}}(\tau)$ is estimating using the IE method. In contrary, when using only the LQG tracking algorithm, $\hat{\bar{\varphi}}(\tau) = 0$is set.

In Eqs. (35)–(38), these equation are dependent on states, $\theta(\tau)$, so we cannot obtain the solution in advance. We solve this problem using an iterative procedure [28]. At first we obtain the state values in the whole interval $[0,\tau_f]$ for the unforced system

$$\begin{aligned}&\dot{\theta}(\tau) = f[\theta(\tau),\bar{\varphi}(\tau),\bar{u}(\tau),\tau] + \omega(\tau), \qquad \bar{\varphi}(\tau) = 0, \quad \bar{u}(\tau) = 0,\\ &\theta(\tau_0) = \theta_0\end{aligned} \tag{40}$$

Now we can solve Eqs. (35)–(38), thus we have $\hat{\bar{u}}(\tau)$ from Eq. (39). Appling this control signal to the system, i.e., Eq. (20), we obtain new state values and again solving Eqs. (35)–(38). This iterative procedure will be checked the deviations of the Kalman gains, such that the value of Kalman gains must satisfy the follow criterion: $|K(k+1) - K(k)| \leqslant 10^{-3}$. The unknown thermal input, $\hat{\bar{\varphi}}(\tau)$, in Eq. (39) can be estimated using the IE method.

The IE algorithm, including the extended Kalman optimal predictor and the weighted recursive least square estimator (WRLSE), will be used to inversely estimate the unknown time-varying heat source and obtain the optimal states estimation in the nonlinear heat conduction problem. The purpose of the extended Kalman optimal predictor is to generate the recursive renewal array. This sequence contains an unknown time-variant heat source. The weighted recursive least square estimator can be used to identify the sudden system error induced by the unknown time-varying heat source.

By sampling Eq. (27) with the sampling time, $\Delta\tau$, the following discrete-time perturbation state equation is obtained:

$$\begin{aligned}\delta\theta(k+1) &= \Phi(k+1,k;*)\delta\theta(k) + \Psi(k+1,k;*)\delta\bar{\varphi}(k)\\ &\quad + \Gamma(k+1,k;*)\delta\bar{u}(k) + \Psi(k+1,k;*)\omega_d(k)\end{aligned} \tag{41}$$

where

$$\Phi(k+1,k;*) \cong I + F_\theta[\theta^*(k),\bar{\varphi}^*(k),\bar{u}^*(k),k]\Delta\tau \tag{41a}$$

$$\Psi(k+1,k;*) \cong F_{\bar{\varphi}}[\theta^*(k),\bar{\varphi}^*(k),\bar{u}^*(k),k]\Delta\tau \tag{41b}$$

$$\Gamma(k+1,k;*) \cong F_{\bar{u}}[\theta^*(k),\bar{\varphi}^*(k),\bar{u}^*(k),k]\Delta\tau \tag{41c}$$

$$F_\theta = \begin{bmatrix} A_{1,1} & A_{1,2} & 0 & \cdots & \cdots & \cdots & 0\\ A_{2,1} & A_{2,2} & A_{2,3} & 0 & \cdots & \cdots & 0\\ & \ddots & \ddots & \ddots & \ddots & & \vdots\\ & \ddots & A_{i,i-1} & A_{i,i} & A_{i,i+1} & & 0\\ & & \ddots & \ddots & \ddots & \ddots & 0\\ 0 & & & 0 & A_{N-1,N-2} & A_{N_1,N-1} & A_{N-1,N}\\ 0 & \cdots & \cdots & \cdots & 0 & A_{N,N-1} & A_{N,N}\end{bmatrix}$$

$$\begin{aligned}A_{1,1} &= \frac{\partial f_1}{\partial\theta_1}\\ &= \frac{2}{h^2}\left[\frac{\bar{C}(\theta_1)(\bar{k}_1 + 2\bar{k}_2\theta_1) - (\bar{c}_1 + 2\bar{c}_2\theta_1)\bar{\kappa}(\theta_1)}{\bar{C}(\theta_1)^2}(\theta_2 - \theta_1)\frac{\bar{\kappa}(\theta_1)}{\bar{C}(\theta_1)^2}\right]\\ &\quad - \frac{(\bar{c} + 2\bar{c}_2\theta_1)\bar{\varphi}(k)\delta(X - X_b)}{\bar{C}(\theta_1)^2}\end{aligned}$$

$$A_{1,2} = \frac{\partial f_1}{\partial\theta_2} = \frac{2}{h^2}\frac{\bar{\kappa}(\theta_1)}{\bar{C}(\theta_1)}$$

$$A_{i,i-1} = \frac{\partial f_i}{\partial\theta_{i-1}}\frac{1}{h^2}\frac{\bar{\kappa}(\theta_i)}{\bar{C}(\theta_i)} + \frac{1}{2h^2}\frac{\bar{k}_1 + 2\bar{k}_2\theta_i}{\bar{C}(\theta_i)}(\theta_{i-1} - \theta_{i+1}),\quad i = 2,\ldots,N-1$$

$$\begin{aligned}A_{i,i}\frac{\partial f_i}{\partial\theta_i} &= \frac{1}{h^2}\left[\frac{\bar{C}(\theta_i)(\bar{k}_1 + 2\bar{k}_2\theta_i) - \bar{\kappa}(\theta_i)(\bar{c}_1 + 2\bar{c}_2\theta_i)}{\bar{C}(\theta_i)^2}(\theta_{i+1} - 2\theta_i + \theta_{i-1}) - 2\frac{\bar{\kappa}(\theta_i)}{\bar{C}(\theta_i)}\right]\\ &\quad + \frac{1}{4h^2}\left[\frac{\bar{C}(\theta_i)2\bar{k}_2 - (\bar{k}_1 + 2\bar{k}_2\theta_i)(\bar{c}_1 + 2\bar{c}_2\theta_i)}{\bar{C}(\theta_i)}(\theta_{i+1} - \theta_{i-1})^2\right]\\ &\quad - \frac{(\bar{c}_1 + 2\bar{c}_2\theta_i)\bar{\varphi}(k)\delta(X - X_b)}{\bar{C}(\theta_i)^2},\ i = 2,\ldots,N\end{aligned}$$

$$A_{i,i+1} = \frac{\partial f_i}{\partial\theta_{i+1}}\frac{1}{h^2}\frac{\bar{\kappa}(\theta_i)}{\bar{C}(\theta_i)} + \frac{1}{2h^2}\frac{\bar{k}_1 + 2\bar{k}_2\theta_i}{\bar{C}(\theta_i)}(\theta_{i+1} - \theta_{i-1}),\quad i = 2,\ldots,N-1$$

$$A_{N,N-1} = \frac{\partial f_N}{\partial\theta_{N-1}} = \frac{2}{h^2}\frac{\bar{\kappa}(\theta_N)}{\bar{C}(\theta_N)}$$

$$A_{N,N}=\frac{\partial f_N}{\partial\theta_N}2h\bar{u}^2\left[\frac{2\bar{k}_2\overline{C}(\theta_N)-(\bar{k}_1+2\bar{k}_2\theta_N)(\bar{c}_1 2\bar{c}_2\theta_N)}{\overline{C}^2(\theta_N)\bar{\kappa}^2(\theta_N)}\right]+\frac{4h(\bar{k}_1+2\bar{k}_2\theta_N)\left[\bar{\kappa}(\theta_N)h\bar{u}-(\bar{k}_1+2\bar{k}_2\theta_N)\bar{u}^2\right]}{\overline{C}(\theta_N)}+\frac{2}{h^2}\left[\frac{\overline{C}(\theta_N)(\bar{k}_1+2\bar{k}_2\theta_N)-(\bar{c}_1+2\bar{c}_2\theta_N)\bar{\kappa}(\theta_N)}{\overline{C}^2(\theta_N)}(\theta_{N-1}-\theta_N)\right]\times\frac{2\bar{\kappa}(\theta_N)}{h^2\overline{C}(\theta_N)}+\frac{2[\bar{u}(\bar{c}_1+2\bar{c}_2\theta_N)]}{h\overline{C}^2(\theta_N)}-\frac{(\bar{c}_1+2\bar{c}_2\theta_N)\bar{\varphi}(k)\delta(X-X_b)}{\overline{C}(\theta_N)^2}$$

$$F_{\bar{\varphi}}[\theta^*(k),\bar{\varphi}^*(k),\bar{u}^*,k]=[0\quad 0\quad\cdots\quad 1\quad\cdots\quad 0\quad 0]^T\times\frac{1}{\overline{C}(\theta_j)}$$

$$F_{\bar{u}}[\theta^*(k),\bar{\varphi}^*(k),\bar{u}^*,k]=[0\quad 0\quad\cdots\quad 0\quad\cdots\quad 0\quad 1]^T\times\left[\frac{4h\bar{u}(\bar{k}_1+2\bar{k}_2\theta_N)}{\overline{C}(\theta_N)\kappa^2(\theta_N)}-\frac{2}{h\overline{C}(\theta_N)}\right]$$

$$\omega_d(k)=\int_{k\Delta\tau}^{(k+1)\Delta\tau}\Phi(k+1,\tau;*)\omega(\tau')d\tau'$$

where $\delta\theta(k)$ represents the state vector, $\Phi(k+1,k;*)$ is the state transition matrix, $\bar{\varphi}(k)$ is the heat source, and $\omega_d(k)$ is a discrete-time Gaussian sequence, which is assumed to be white noise with zero mean and the variance, $\{\omega_d(k)\omega_d^T(j)\}=Q_d\delta_{kj}$, where δ_{kj} is the Dirac delta function. The discrete-time measurement equation is shown below.

$$z_(k)=H\theta(k)+v(k) \tag{42}$$

$z(k)$ represents the measurement vector at kth time step $H=[0\quad 0\quad\cdots\quad 1]$ is the measurement matrix. $v(k)$ is the Gaussian white noise with zero mean and the variance, $E\{v(k)v^T(j)\}=R\delta_{kj}$.

The extended Kalman optimal predictor is defined as follows [29]:

$$\hat{\theta}(k+1/k)=\hat{\theta}(k/k-1)+\int_{k\Delta\tau}^{(k+1)\Delta}f\left[\hat{\theta}(k/k-1),\bar{\varphi}^*(k)\hat{\bar{u}}^*,\tau\right]d\tau+K(k;*)\bar{z}(k) \tag{43}$$

$$\bar{z}=z(k)-H\hat{\theta}(k/k-1) \tag{44}$$

$$s(k)=[H(k;*)P(k/k-1;*)H^T(k;*)+R(k)]^{-1} \tag{45}$$

$$K(k;*)=\Phi(k+1/k)P(k/k-1;*)H^T(k;*)s(k) \tag{46}$$

$$P(k+1/k;*)=\Phi(k+1/k;*)P(k/k-1;*)\Phi^T(k+1/k;*)-\Phi(k+1/k;*)P(k/k-1;*)H^T(k,*)\times[H^T(k;*)P(k/k-1;*)H^T(k,*)+R]^{-1}H(k;*)P(k/k-1;*)\Phi^T(k+1/k;*)+Q_d(k+1/k;*) \tag{47}$$

where $\hat{\theta}(k+1/k)$ is the optimal states prediction. $\int_{k\Delta\tau}^{(k+1)\Delta}f\left[\hat{\theta}(k/k-1),\bar{\varphi}^*(k)\hat{\bar{u}}^*,\tau\right]$ is evaluated using numerical integration formulas that are initialized by $f\left[\hat{\theta}(k/k-1),\bar{\varphi}^*(k),\hat{\bar{u}}^*,\tau\right]$. $s(k)$ is the covariance of the residual. $K(k)$ is the Kalman gain. In Eqs. (43)–(47), $*$ denotes the use of $\theta^*(k)=\hat{\theta}(k/k-1)$.

The weighed recursive least square estimator was proposed by Tuan et al. [14]. The mathematical equations are described briefly below:

$$B(k)=H[\Phi M(k-1)+I\Psi] \tag{48}$$

$$M(k)=[I-K(k)H][\Phi M(k-1)+I] \tag{49}$$

$$K_b(k)=\gamma^{-1}P_b(k-1)B^T(k)[B(k)\gamma^{-1}P_b(k-1)B^T(k)+s(k)]^{-1} \tag{50}$$

$$P_b(k)=[I-K_b(k)B(k)]\gamma^{-1}P_b(k-1) \tag{51}$$

$$\hat{\bar{\varphi}}(k)=\hat{\bar{\varphi}}(k-1)+K_b(k)\left[\bar{z}(k)-B(k)\hat{\bar{\varphi}}(k-1)\right] \tag{52}$$

where $\hat{\bar{\varphi}}(k)$ is the estimated unknown heat source, $P_b(k)$ is the error covariance of the estimated input vector, $B(k)$ and $M(k)$ are the sensitivity matrices, and $K_b(k)$ is the Kalman gain. $\bar{z}(k)$ is the bias input error caused by the measurement noise and input disturbance. In this case, the correction gain $K_b(k)$ for updating $\hat{\bar{\varphi}}(k)$ in Eq. (52) diminishes as k increases, and permits $\hat{\bar{\varphi}}(k)$ to converge to the true constant value. In the time-varying case, however, we like to prevent $K_b(k)$ from reducing to zero. This is accomplished by introducing the memory factor γ. For, $0<\gamma\leqslant 1$, $K_b(k)$ is effectively prevented from shrinking to zero. Hence, the corresponding algorithm can continuously preserve its updating ability. The γ value depends on the process noise covariance Q and the measurement noise covariance R. Usually, the R value depends on the sensor measurements. Both the Q value in the filter and the γ value in the sequential least squares approach will interactively affect the fast adaptive capability in tracking of time-varying heat generated by the semiconductor chip. In general, if we select a large Q value, the γ value could be chosen near 1 and the filter memory becomes long, reducing the noise effects. For a smaller γ value, the memory becomes short and the estimation can track sudden changes occurring in the heat flux, $\hat{\bar{\varphi}}(k)$.

To simulate measurement temperature of the thermal conductor of package seal under heating, $\bar{\varphi}_{exact}(\tau)$, and the amount of heat which must be dissipated, $\hat{\bar{u}},\tau$, the system response equation is as follows:

$$\dot{\theta}(\tau)=f\left[\theta(\tau),\varphi_{exact}(\tau),\hat{\bar{u}},\tau\right] \tag{53}$$

In order to verify the performance of the controller, the root mean square error (RMSE) is defined.

$$\mathrm{RMSE}=\left[\frac{1}{k_f}\sum_{k=1}^{k_f}\left[\theta_d(k)-\theta_p(k)\right]^2\right]^{\frac{1}{2}} \tag{54}$$

Fig. 3 presents a detailed control flow chart of the LQG/IE tracking algorithm.

4. Results and discussion

In order to verify the effectiveness and precision of the heat source estimation and the optimal heat dissipation implemented in the nonlinear heat conduction system by the LQG/IE tracking algorithm. Assume the thermal conductivity coefficient, $\bar{\kappa}=$

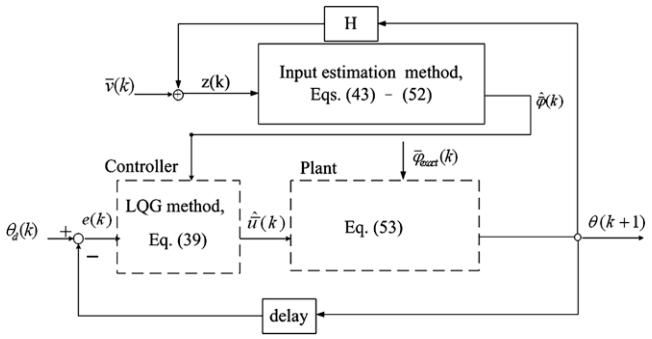

Fig. 3. LQG/IE control flow chart.

$1 - 0.0052\theta + 0.00002235\theta^2$, and the volumetric heat capacity, $\overline{C} = 1 + 0.0088\theta - 0.0000425\theta^2$. The electronic component is divided into 10 sections. Each section has length, $h = 0.1$. That is to say, there are 11 nodes from $X = 0$ to $X = 1$. One end of the system is thermal isolated, and the other is in compulsory convection condition. Assume that the sampling time, $\Delta\tau = 0.001$. The initial conditions of the extended Kalman optimal predictor are as follows. $\hat{\theta}(1/0) = [1 \quad 1 \quad \cdots \quad 1]^T, Q_d = \mathrm{diag}[10^{-8}]$, and $P(1/0) = \mathrm{diag}[10^2]$. The initial conditions of the WRLSE are as follows: $\hat{\bar{\varphi}}(0) = 0, P_b(0) = 10^2$ and $M(0) = 0$. The weighted factor, γ, is set to be 0.975. The parameters of the LQG tracking algorithm are $Q_s = \mathrm{diag}[0.1]$. The initial optimal control input $\bar{u}(0) = 0$ is assumed.

Based on a guessed value for $\bar{\varphi}_{exact}(\tau)$ of the heat source generated by the electronic device and a computation of the amount of heat which must be dissipated, $\hat{\bar{u}}(\tau)$, using the LQG tracking algorithm, the distribution of the temperature field can be determined using the direct heat conduction method from Eq. (53). Furthermore, the measurement error can be added to the determined temperature field to yield the measurement temperature.

$$z(\tau) = \theta(X, \tau) + \eta\sigma, \quad X = 1 \tag{55}$$

where η is a random variable in the range $-2.576 \leqslant \eta \leqslant 2.576$ and $\boldsymbol{\sigma}$ denotes the standard deviation of the measurements. By assuming that there is a thermocouple embedded on the top of the package seal at $X = 1$, the simulated measurement temperature can be determined. The estimation and optimal thermal control is implemented by applying two time-varying heat source models as in case 1 and case 2. The results are compared with those obtained using the LQG tracking algorithm.*Case 1*: The strength of the heat source is assumed to be a square wave and acting on node 6.

$$\bar{\varphi}_1(\tau) = \begin{cases} 10 & 10 \leqslant \tau < 23 \\ 0 & \text{others} \end{cases} \tag{56}$$

The measurement noise covariance, $R = 0.0001$, weights of the control, $Q_c = 0.01$, and design working temperature, $\theta_d(\tau) = 3$, are considered. Fig. 4 presents the inverse estimation of the square heat source wave using the IE method, indicating that the IE method can effectively estimate the unknown time-varying heat source in real time based on simulated temperature measurement. As indicated in Fig. 4, the oscillations during the initial time steps are very large, but for a few time steps the estimates rapidly converge to their actual values. The main reason is that the initial value of $P(-1/-1)$ and $P_b(-1)$ are normally unknown and the initial error is assumed to be large enough that it causes the estimator to converge rapidly within a short transition period and steadily track the actual values. This shows that the proposed technique is capable of correcting the initial estimation error using very large values for $P(-1/-1)$ and $P_b(-1)$. Fig. 5 presents the optimal control heat-flux results, revealing that the LQG/IE tracking algorithm can provide a short time response and more precise tracking than that obtained using only the LQG tracking algorithm. To compare the control performance for the various control algorithms, the temperature of package seal near the chip is calculated. As shown in Fig. 6, the LQG tracking algorithm reacts more slowly then the LQG/IE tracking algorithm and larger overshoot between the maximum temperature of package seal near the chip and design working temperature. This error arises from the fact that the LQG tracking algorithm cannot recognize when an unknown thermal input acts on the thermal conductor. The IE method, however, can estimate an unknown thermal input in real time. Combining the IE method and the LQG tracking algorithm, which computes the optimal thermal control heat flux, can yield rapid and precise heat-dissipation results. The RMSE value based on the LQG tracking algorithm is 2.48×10^{-2} and based on LQG/IE tracking algorithm, the value is 2.55×10^{-4}. Therefore, the LQG/IE tracking algorithm can maintain a universal system temperature within an ideal range and is suited to heat-dissipation applications in unknown systems with time-varying or transient thermal input sources.

To examine the control performance of the various algorithms with larger weights on the control effort, $Q_c = 0.1$, is assumed. Comparisons of the heat dissipation results using the LQG/IE tracking algorithm and the LQG tracking algorithm are shown in Figs. 5 and 7. It is interesting to point out, when we adjusted a larger value, Q_c, the function frequency of the heat dissipation controller was then enhanced. The means that a larger Q_c value is the smaller value of the maximum heat dissipating capacity, $\bar{u}_{\max}$, can be provided by the cooling system. The temperature of the package seal near the chip obtained using the LQG/IE tracking algorithm and

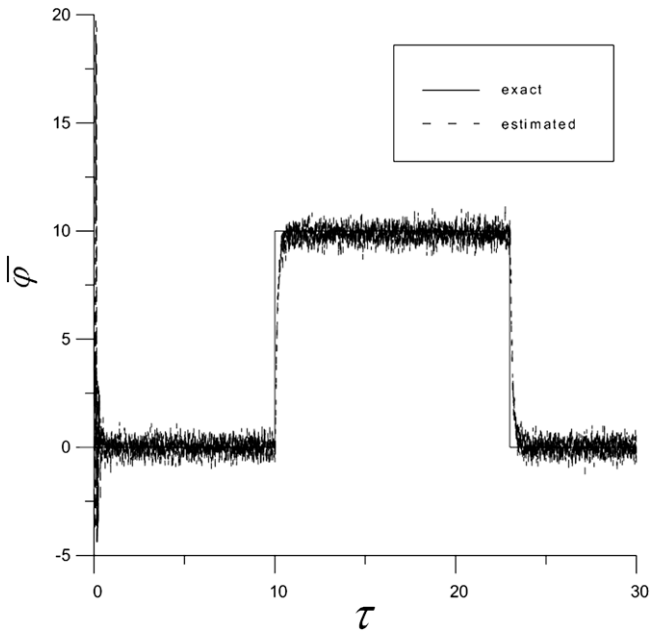

Fig. 4. Estimated heat flux using IE algorithm for Case 1 ($R = 10^{-4}$).

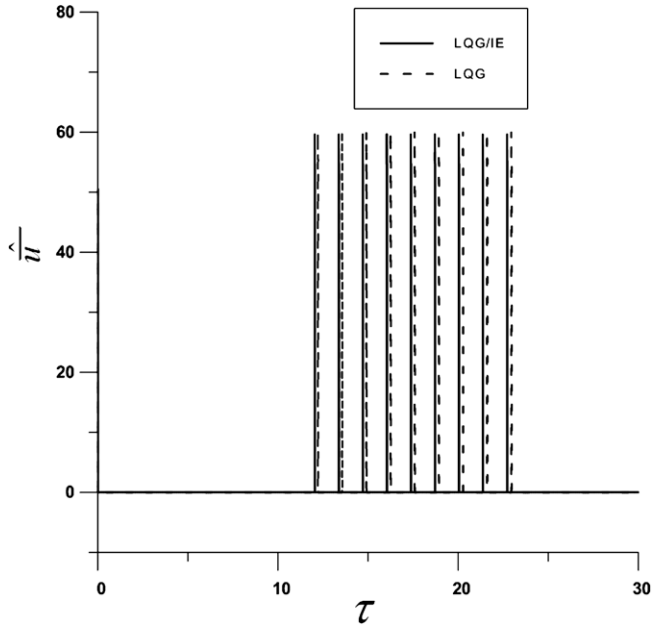

Fig. 5. Dissipative heat flux for various control algorithms for Case 1 ($R = 10^{-4}$, $Q_c = 0.01$).

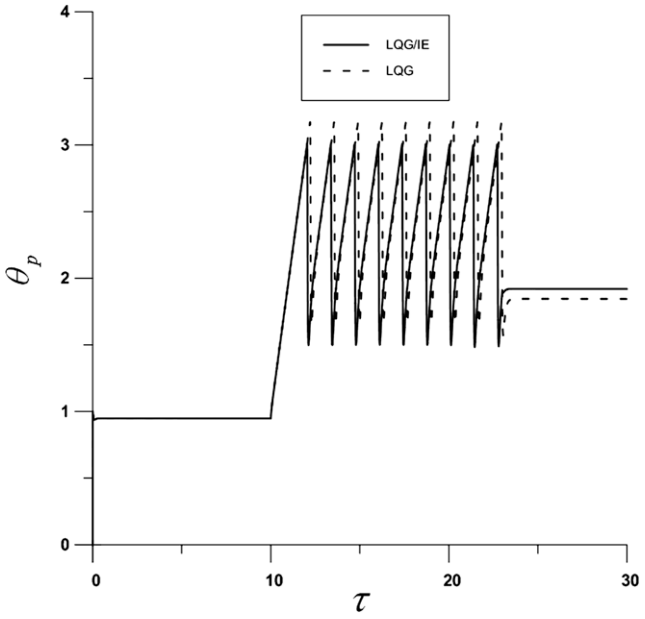

Fig. 6. Comparison of temperature of package seal near the chip using various control algorithms for Case 1 ($R = 10^{-4}$, $Q_c = 0.01$).

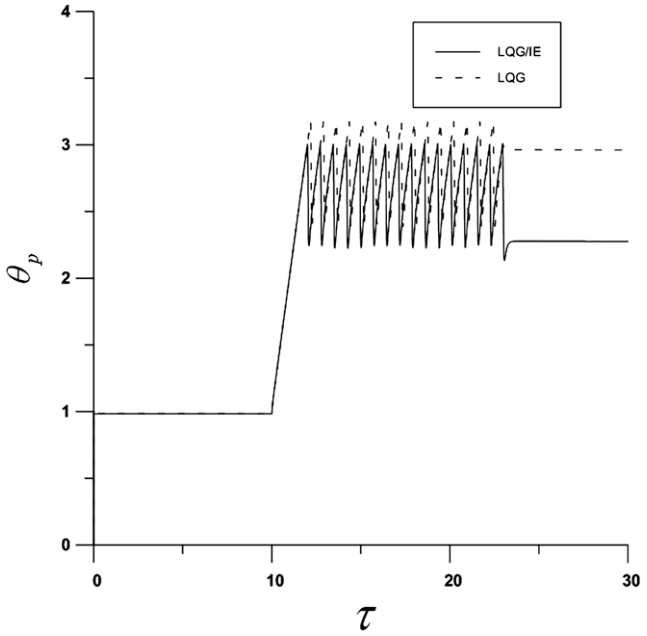

Fig. 8. Comparison of temperature of package seal near the chip using various control algorithms for Case 1 ($R = 10^{-4}$, $Q_c = 0.1$).

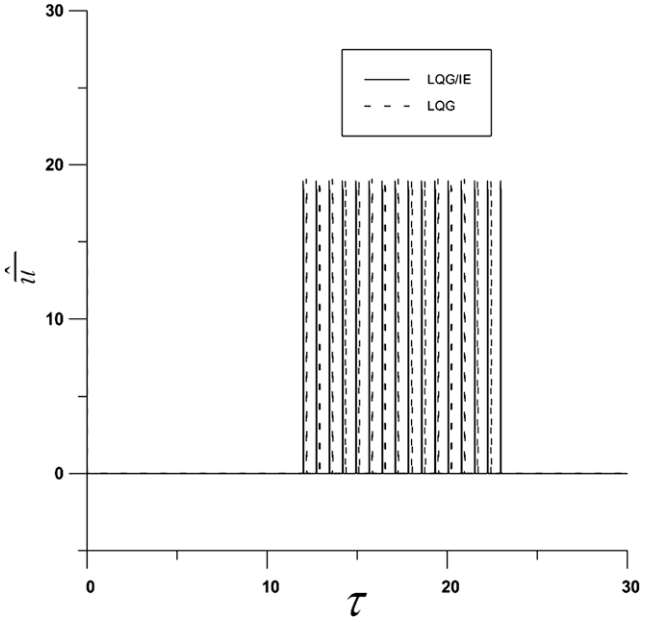

Fig. 7. Dissipative heat flux for various control algorithms for Case 1($R = 10^{-4}$, $Q_c = 0.1$).

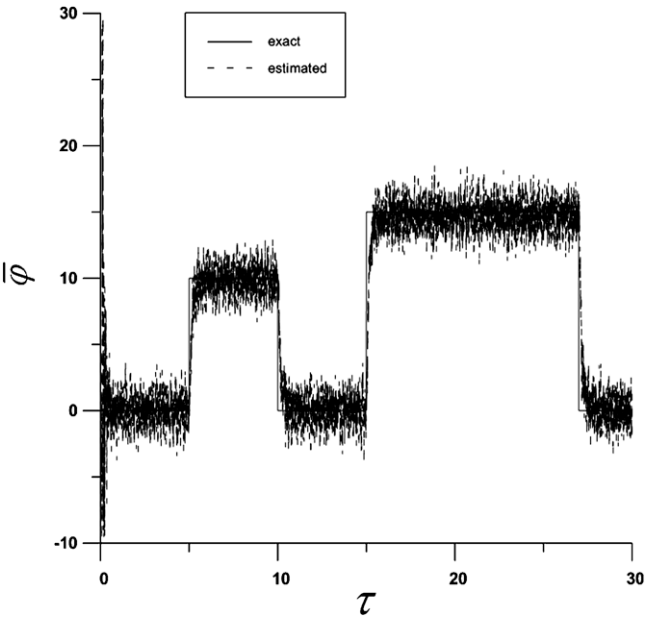

Fig. 9. Estimated heat flux using IE algorithm for Case 2 ($R = 10^{-3}$).

the LQG tracking algorithm are shown in Fig. 8. These results are consistent with the results in Fig. 6. The RMSE value based on the LQG tracking algorithm is 3.33×10^{-2} and based on LQG/IE tracking algorithm, the value is 5.19×10^{-4}.

Case 2: The strength of heat source is assumed as a compound square wave.

Suppose that the time-varying heat source input is

$$\bar{\varphi}_2(\tau) = \begin{cases} 10 & 5 \leqslant \tau < 10 \\ 15 & 15 \leqslant \tau < 27 \\ 0 & \text{others} \end{cases} \tag{57}$$

The second case is the same as that considered in the first, except that the covariances of measurement noise, $R = 0.001$. Fig. 9 depicts inverse estimation of a compound square heat source wave using the IE method and verifies that the IE method with the simulated temperature can effectively estimate the unknown time-varying heat source in real time. The control weights are set to $Q_c = 0.01$. Fig. 10 presents the optimal control heat-flux results. Fig. 11 presents the temperature profile of the package seal near the chip after control. The RMSE value based on the LQG tracking algorithm is 2.45×10^{-2} and based on LQG/IE tracking algorithm, the value is 3.23×10^{-4}. When we adjust a larger value, $Q_c = 0.1$, the optimal control heat-flux re-

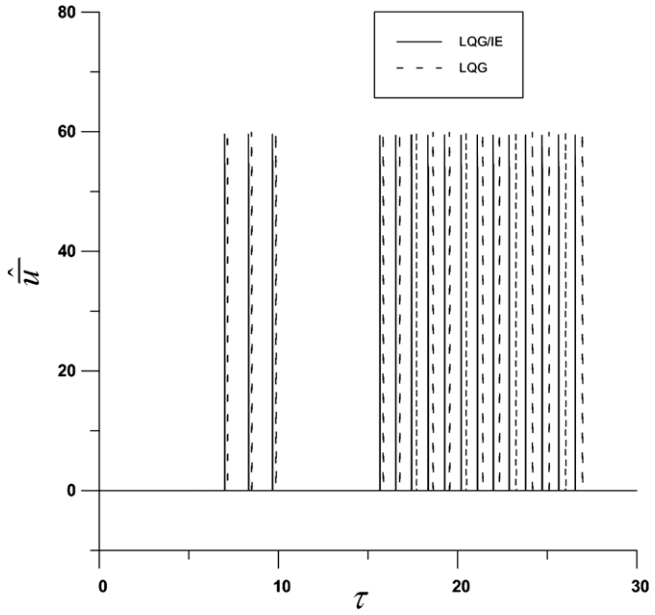

Fig. 10. Dissipative heat flux for various control algorithms for Case 2 ($R = 10^{-3}$, $Q_c = 0.01$).

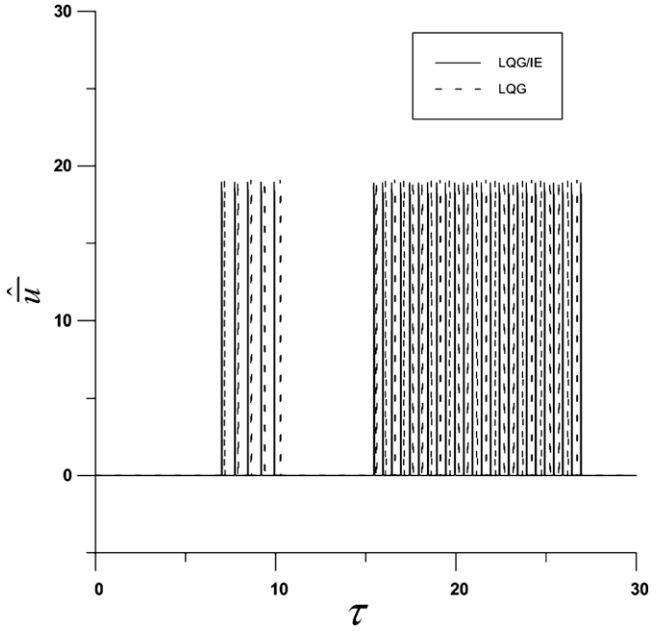

Fig. 12. Dissipative heat flux for various control algorithms for Case 2 ($R = 10^{-3}$, $Q_c = 0.1$).

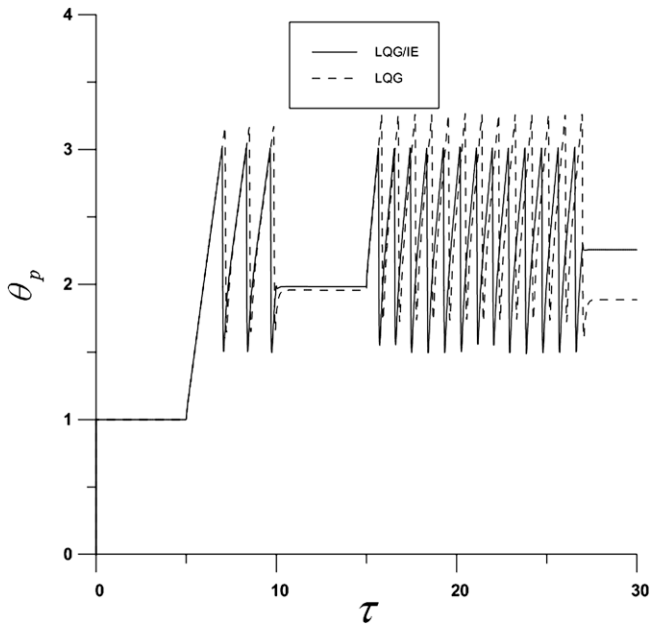

Fig. 11. Comparison of temperature of package seal near chip using various control algorithms for Case 2 ($R = 10^{-3}$, $Q_c = 0.01$).

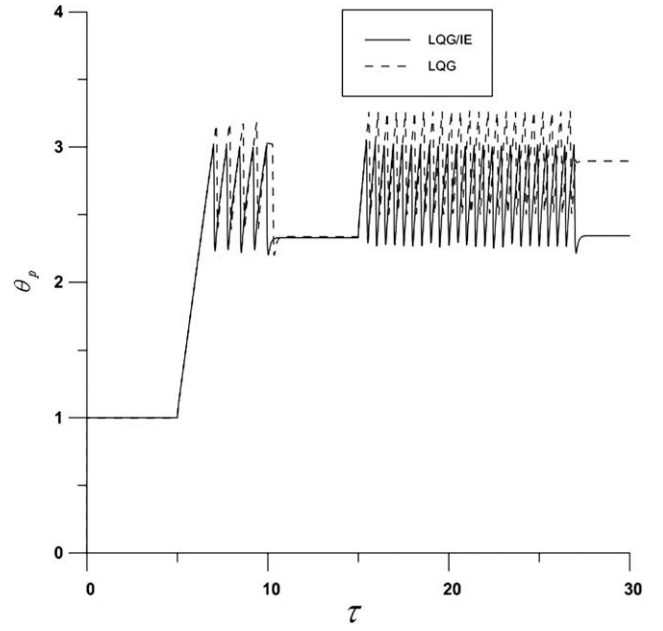

Fig. 13. Comparison of temperature of package seal near the chip using various control algorithms for Case 2 ($R = 10^{-3}$, $Q_c = 0.1$).

sults shown in Fig. 12 and the temperature profile of nearing the chip position obtained using the LQG/IE tracking algorithm and the LQG tracking algorithm shown in Fig. 13. The RMSE value based on the LQG tracking algorithm is 3.32×10^{-2} and based on LQG/IE tracking algorithm, the value is 5.59×10^{-4}. All of these results are consistent with the discussion on Case 1. The LQG/IE tracking algorithm yields a shorter response time and more precise outcome than the LQG regulator.

5. Conclusions

In this article, a nonlinear optimal on-line heat-dissipation control methodology in electronic devices, based on IE method and LQG tracking algorithm, is developed for predicting the optimal value of time-varying heat dissipation which must be removed by the cooling system, with the problem corrupted by modeling noise and unknown thermal input. From the computer simulation studies, we have demonstrated that the LQG/IE tracking algorithm outperforms the LQG tracking algorithm with a shorter response time and more accurate heat flux tracking. Therefore, optimal heat-dissipation control using an LQG/IE algorithm can provide time-varying heat dissipation which can be used to design an effective cooling system to assure that electronic devices operate within a safe temperature regime. Further work will involve implementing the LQG/IE algorithm in electronic devices.

References

[1] S.V. Garimella, Y.K. Joshi, A. Bar-Cohen, R. Mahajan, K.C. Toh, V.P. Carey, M. Baelmans, J. Lohan, B. Sammakia, F. Andros, Thermal challenges in next generation electronic systems- summary of panel presentations and discussions, Institute of Electrical and Electronic Engineers, Trans. Component Packag. Technol. 25 (4) (2002) 569–575.

[2] R.R. Tummala, E.J. Rymaszewski, Microelectronic Packaging Handbook, van Nostrad–Reinhold, New York, 1989. pp. 385–390.

[3] P. Mithal, Design of experimental based evaluation of thermal performance of a chip electronic assembly, in American Society of Mechanical Engineers, Sensing Modeling and Simulation in Emerging Electronic Packaging Proceedings, New York, vol. 18, 1996, pp. 109–115.

[4] A.H. Charles, Electronic Materials and Processes Handbook, third ed., McGraw-Hill, New York, 2004.

[5] R. Viswanath, V. Wakharkar, A. Watwe, V. Lebonheur, Thermal performance challenges from silicon to system, Intel Technol. J. 3 (2000) 9–25.

[6] Bar-Cohen. Avram, W.B. Krueger, Thermal characterization of chip packages – evolutionary development of compact models, in: Institute of Electrical and Electronic Engineers, Trans. Component. Packag. Manuf. Technol. A 20 (4) (1997) 399–410.

[7] T. Kobayashi, T. Ogushi, N. Sumi, M. Fujii, Thermal design of a ultra-slim notebook computer, in: Institute of Electrical and Electronic Engineers, Thermal and Thermomechanical Phenomena in Electronic Systems, The Sixth InterSociety Conference on Thermal Phenomena, 1998, pp.15–21.

[8] T. Branchaud, Thermal modeling techniques for heat sinks for power electronics, in: Applied Power Electronics Conference and Exposition, vol. 1, 1997, pp. 424–428.

[9] C. Lundquist, V.P. Carey, Microprocessor-based adaptive thermal control for an air-cooled computer CPU module, in: Semiconductor Thermal Measurement and Management, Seventeenth Annual Institute of Electrical and Electronic Engineers Symposium, 2001, pp. 168–173.

[10] D.A. Murdock, J.E.R. Torres, J.J. Connors, R.D. Lorenz, Active thermal control of power electronic modules, Institute of Electrical and Electronic Engineers, Trans. Ind. Appl. 42 (2) (2006).

[11] M. Malinoski, J. Maveety, S. Knostman, T. Jones, A test site thermal control system for at-speed manufacturing testing, in: Proceedings of the Institute of Electrical and Electronic Engineers, International Test Conference, 1998, pp. 119–128.

[12] A.C. Pfahnl,, J.H. Lienhard V, A.H. Slocum, Temperature control of a handler test interface, in Proceedings of the Institute of Electrical and Electronic Engineers, International Test Conference, 1998, pp.114–118.

[13] J.B. Burl, Linear Optimal Control: H_2 and H_∞ methods, Linear Quadratic Gaussian Control, Addison-Wesley–Longman, California, 1998. pp. 280–310.

[14] P.C. Tuan, C.C. Ji, L.W. Fong, W.T. Huang, An input estimation approach to on-line two-dimensional inverse heat conduction problems, Numer. Heat Transfer B 29 (1996) 345–363.

[15] P.C. Tuan, L.W. Fong, W.T. Huang, Application of Kalman filtering with input estimation technique to on-line cylindrical inverse heat conduction problems, J. Jpn. Soc. Mech. Eng. Int. J. Ser. B 40 (1) (1997) 126–133.

[16] C.C. Ji, P.C. Tuan, H.Y. Jang, A recursive least-squares algorithm for on-line 1-D inverse heat conduction estimation, Int. J. Heat Mass Transfer 40 (9) (1997) 2081–2096.

[17] R.A. Meric, Finite element and conjugate gradient methods for a nonlinear optimal heat transfer control problem, Int. J. Numer. Meth. Eng. 14 (1979) 1851–1863.

[18] R.A. Meric, Finite element analysis of optimal heating of a slab with temperature dependent thermal conductivity, Int. J. Heat Mass Transfer 22 (1979) 1347–1353.

[19] C.J. Chen, M.N. Ozisik, Optimal heating of a slab with a plane heat source of timewise varying strength, Numer. Heat Transfer A 21 (1992) 351–361.

[20] C.J. Chen, M.N. Ozisik, Optimal heating of a slab with two plane heat source of timewise varying strength, J. Franklin Inst. 329 (1992) 195–206.

[21] C.J. Chen, M.N. Ozisik, Optimal convective heating of a hollow cylinder with temperature dependent thermal conductivity, Appl. Sci. Res. 52 (1994) 67–79.

[22] C.H. Huang, A non-linear optimal control problem in determining the strength of the optimal boundary heat fluxes, Numer. Heat Transfer B 40 (2001) 411–429.

[23] N. Daouas, M.S. Radhouani, A new approach of the Kalman filter using future temperature measurement for nonlinear inverse heat conduction problems, Numer. Heat Transfer B 45 (2004) 565–585.

[24] H.T. Chen, X.Y. Wu, Estimation of surface conditions for nonlinear inverse heat conduction problems using the hybrid inverse scheme, Numer. Heat Transfer B 51 (2007) 159–178.

[25] T. Loulou, E. Artioukhine, Numerical solution of 3D unsteady nonlinear inverse problem of estimating surface heat flux for cylindrical geometry, Inverse Probl. Sci. Eng. 14 (1) (2006) 39–52.

[26] T.C. Chen, C.H. Cheng, H.Y. Jang, P.C. Tuan, Using input estimation to estimate heat source in nonlinear heat conduction problem, J. Thermophys. Heat Transfer 21 (1) (2007) 166–172.

[27] N. D'Souza, Numerical solution of one-dimensional inverse transient heat conduction by finite difference method, American Society of Mechanical Engineers, Paper 75-WA/HT-81, 1975.

[28] P. Dorato, A. Levis, Optimal linear regulator: the discrete time case, Institute of Electrical and Electronic Engineers, Trans. Automat. Control 16 (1970) 613–620.

[29] J.M. Mendel, Lessons in Estimation Theory for Signal Processing, Communications and Control, Prentice-Hall PTR, Englewood Cliffs, NJ, 1995. pp. 384–394.